

# Low-complexity Image and Video Coding Based on an Approximate Discrete Tchebichef Transform

Paulo A. M. Oliveira\* Renato J. Cintra† Fábio M. Bayer‡ Sunera Kulasekera§ Arjuna Madanayake§  
 Vítor A. Coutinho ¶

## Abstract

The usage of linear transformations has great relevance for data decorrelation applications, like image and video compression. In that sense, the discrete Tchebichef transform (DTT) possesses useful coding and decorrelation properties. The DTT transform kernel does not depend on the input data and fast algorithms can be developed to real time applications. However, the DTT fast algorithm presented in literature possess high computational complexity. In this work, we introduce a new low-complexity approximation for the DTT. The fast algorithm of the proposed transform is multiplication-free and requires a reduced number of additions and bit-shifting operations. Image and video compression simulations in popular standards shows good performance of the proposed transform. Regarding hardware resource consumption for FPGA shows 43.1% reduction of configurable logic blocks and ASIC place and route realization shows 57.7% reduction in the area-time figure when compared with the 2-D version of the exact DTT.

## Keywords

Approximate transforms, discrete Tchebichef transform, fast algorithms, image and video coding

## 1 INTRODUCTION

Discrete variable orthogonal polynomials emerge as solutions of several hypergeometric difference equations [1]. Classic applications of this class of orthogonal polynomials include functional analysis [2] and graphs [3]. Additionally, such polynomials are employed in the computation of moment functions [4], which are largely used in image processing [5–7]. For instance, the discrete Tchebichef moments [8], which are derived from the discrete Tchebichef polynomials, form a set of orthogonal moment functions. Such functions are not discrete approximation based on continuous functions; they are naturally orthogonal over the discrete domain.

The Tchebichef moments have been used for quantifying image block artifact [9], image recognition [10–12], blind integrity verification [13], and image compression [14–18]. In the data compression context, bi-dimensional (2-D) moments are computed by means of the 2-D discrete Tchebichef transform (DTT). In fact, the 8-point DTT can achieve better performance when comparison with the discrete cosine transform (DCT) [19], in terms of average bit length as reported in [16, 20, 21]. Moreover, the 8-point DTT-based embedded encoder proposed in [18], shows improved image quality and reduced encoding/decoding time in comparison with state-of-the-art DCT-based embedded coders. The 8-point DTT has also been employed in blind forensics, as a tool to determine the integrity of medical imagery subject to

filtering and compression [13].

However, the exact DTT possesses high arithmetic complexity, due to its significant amount of additions and float-point multiplications. Such multiplications are known to be more demanding computational structures than additions or fixed-point multiplications, both in *software* and *hardware*. Thus, the higher computational complexity of the DTT precludes its applications in low power consumption systems [22, 23] and/or real-time processing, such as video streaming [24, 25]. Therefore, fast algorithms for the DTT could improve its computational efficiency. A comprehensive literature search reveals only two fast algorithms for the 4-point DTT [14, 26] and one for the 8-point DTT [15]. Although these fast algorithms possess lower arithmetic complexities when compared with the direct DTT calculation, they still possess high arithmetic complexity, requiring a significant amount of additions and bit-shifting operations.

In a comparable scenario, the computation of DCT-based transforms—which has been employed in several popular coding schemes such as JPEG [27], MPEG-2 [28], H.261 [29], H.263 [30], H.264 [31], HEVC [32, 33], and VP9 [34]—has profited from matrix approximation theory [35–41]. In this context, discrete transforms are not exactly calculated, but instead an approximate, low-cost computation, is performed. The approximations are designed in such a way to allow similar spectral and coding characteristics as well as lower arithmetic complexity. Usually, approximations are multiplierless, requiring only addition and bit-shifting operations for its computation. In [42], a multiplierless approximation for the 8-point DTT is proposed. To the best of our knowledge, this is the only DTT approximation archived in literature.

The aim of this work is to introduce an efficient low-complexity approximation for the 8-point DTT capable of outperforming [42]. To derive multiplierless approximate DTT matrix, a multicriteria optimization problem is sought, combining different coding metrics: coding gain and transform efficiency. Additionally, a fast algorithm for efficient computation of the sought approximation is also pursued. For coding performance evaluation, we propose two computational experiments: (i) a JPEG image compression simulation and (ii) a video coding experiment

\*Paulo A. M. Oliveira is with the Signal Processing Group, Departamento de Estatística, Universidade Federal de Pernambuco, Recife, PE, Brazil; Multimedia Communications and Signal Processing, University of Erlangen–Nuremberg, Erlangen, BY, Germany.

†Renato J. Cintra is with the Signal Processing Group, Departamento de Estatística, Universidade Federal de Pernambuco, Recife, PE, Brazil; Equipe Cairn, INRIA-IRISA, Université de Rennes, Rennes, France; and LIRIS, Institut National des Sciences Appliquées, Lyon, France (e-mail: rjpsc@dsp.ufpe.org).

‡Fábio M. Bayer is with the Departamento de Estatística and LACESM, Universidade Federal de Santa Maria, Santa Maria, RS, Brazil (e-mail: bayer@ufsm.br).

§Sunera Kulasekera and Arjuna Madanayake are with the Department of Electrical and Computer Engineering at the University of Akron, OH (e-mail: arjuna@uakron.edu).

¶Vítor A. Coutinho is with the Signal Processing Group, Departamento de Estatística, UFPE, Recife, Brazil. (e-mail: vdacl@de.ufpe.br)

which consists of embedding the sought approximation into the H.264/AVC standard.

The paper unfolds as follows. Section 2 reviews the mathematical background of the DTT. Section 3 introduces a parametrization of the DTT to derive a family of DTT approximations and sets up an optimization problem to identify optimal approximations. In Section 4, we assess the obtained approximation in terms of coding performance, proximity with the exact transform, and computation cost. Moreover, a fast algorithm for the proposed approximate DTT is introduced. Section 5 shows the results of the image and video compression simulations. Section 6 shows hardware resource consumption comparison with the exact DTT for both FPGA and ASIC realizations. A discussion and final remarks are shown in Section 7.

## 2 DISCRETE TCHEBICHEF TRANSFORM

### 2.1 DISCRETE TCHEBICHEF POLYNOMIALS

The discrete Tchebichef polynomials are a set of discrete variable orthogonal polynomials [43]. The  $k$ th order discrete Tchebichef polynomials are given by the following closed form expression [14]:

$$t_k[n] = (1 - N)_k \cdot {}_3F_2(-k, -n, 1 + k; 1, 1 - N; 1),$$

where  $n = 0, 1, \dots, N - 1$ ,  ${}_3F_2(a_1, a_2, a_3; b_1, b_2; z) = \sum_{n=0}^{\infty} \frac{(a_1)_n (a_2)_n (a_3)_n z^n}{(b_1)_n (b_2)_n n!}$  is the generalized hypergeometric function and  $(a)_k = a(a+1) \cdots (a+k-1)$  is the descendant factorial. Tchebichef polynomials can be obtained according to the following recursion [14]:

$$t_k[n] = \left[ \frac{2k-1}{k} t_k[1] \right] t_{k-1}[n] - \left[ \frac{k-1}{k} (N^2 - (k-1)^2) \right] t_{k-2}[n],$$

for  $t_0[n] = 1$  and  $t_1[n] = 2n - N + 1$ . Indeed, the set  $\{t_k[n]\}$ ,  $k = 0, 1, \dots, N - 1$ , is an orthogonal basis in respect with the unit weight. Consequently, the discrete Tchebichef polynomials satisfy the following mathematical relation:

$$\sum_{i=0}^{N-1} t_i[n] t_j[n] = \rho(j, N) \cdot \delta_{i,j},$$

where  $\rho(k, N) = \frac{(N+k)!}{(2k+1) \cdot (N-k-1)!}$  and  $\delta_{i,j}$  is the Kronecker delta function which yields  $\delta_{i,j} = 1$ , if  $i = j$ , and  $\delta_{i,j} = 0$ , otherwise.

### 2.2 2-D DISCRETE TCHEBICHEF TRANSFORM

Let  $\mathbf{f}[m, n]$ ,  $m, n = 0, 1, \dots, N - 1$ , be an intensity distribution from a discrete image of size  $N \times N$  pixels. The 2-D DTT of  $\mathbf{f}[m, n]$ , denoted by  $\mathbf{M}[p, q]$ ,  $p, q = 0, 1, \dots, N - 1$ , is given by [8, 14]:

$$\mathbf{M}[p, q] = \sum_{m,n=0}^{N-1} \tilde{t}_p[m] \cdot \tilde{t}_q[n] \cdot \mathbf{f}[m, n], \quad (1)$$

where  $\tilde{t}_k[n]$ ,  $k = 0, 1, \dots, N - 1$ , are the orthonormalized discrete Tchebichef polynomials given by  $\tilde{t}_k[n] = t_k[n] / \sqrt{\rho(k, N)}$ .

Note that the transform kernel described in (1) is separable. Hence, the following is relation holds true:

$$\mathbf{M}[p, q] = \sum_{m=0}^{N-1} \tilde{t}_p[m] \sum_{n=0}^{N-1} \tilde{t}_q[n] \cdot \mathbf{f}[m, n],$$

for  $p, q = 0, 1, \dots, N - 1$ . Therefore, the transform-domain coefficients of  $\mathbf{f}$  can be calculated by the following matrix operation:

$$\mathbf{M} = \mathbf{T} \cdot \mathbf{f} \cdot \mathbf{T}^\top, \quad (2)$$

where  $\mathbf{T}$  is the  $N$ -point unidimensional DTT matrix given by

$$\mathbf{T} = \begin{bmatrix} \tilde{t}_0[0] & \tilde{t}_0[1] & \cdots & \tilde{t}_0[N-1] \\ \tilde{t}_1[0] & \tilde{t}_1[1] & \cdots & \tilde{t}_1[N-1] \\ \vdots & \vdots & \ddots & \vdots \\ \tilde{t}_{N-1}[0] & \tilde{t}_{N-1}[1] & \cdots & \tilde{t}_{N-1}[N-1] \end{bmatrix}.$$

The matrix operations induced by (2) represents the 2-D DTT. Because of the kernel separation property, the 2-D DTT can be calculated by means the successive applications of the 1-D DTT to the rows of  $\mathbf{f}$ ; and then to columns of the resulting intermediate matrix. The original intensity distribution  $\mathbf{f}$  can be recovered by the inverse procedure:

$$\mathbf{f} = \mathbf{T}^{-1} \cdot \mathbf{M} \cdot (\mathbf{T}^{-1})^\top = \mathbf{T}^\top \cdot \mathbf{M} \cdot \mathbf{T}.$$

The last equality above stems from the DTT orthogonality property:  $\mathbf{T}^\top = \mathbf{T}^{-1}$  [14]. Therefore, the same structure can be used at the forward transform as well in the inverse.

For  $N = 4$  and  $N = 8$ , we have the particular cases of interest in the context of image and video coding. Thus, the 4- and 8-point DTT matrices are, respectively, furnished by:

$$\mathbf{T}_4 = \mathbf{F}_4 \cdot \begin{bmatrix} 1 & 1 & 1 & 1 \\ -3 & -1 & 1 & 3 \\ 1 & -1 & -1 & 1 \\ -1 & 3 & -3 & 1 \end{bmatrix}$$

and

$$\mathbf{T}_8 = \frac{1}{2} \cdot \mathbf{F}_8 \cdot \begin{bmatrix} 1 & 1 & 1 & 1 & 1 & 1 & 1 & 1 \\ -7 & -5 & -3 & -1 & 1 & 3 & 5 & 7 \\ 7 & 1 & -3 & -5 & -5 & -3 & 1 & 7 \\ -7 & 5 & 7 & 3 & -3 & -7 & -5 & 7 \\ 7 & -13 & -3 & 9 & 9 & -3 & -13 & 7 \\ -7 & 23 & -17 & -15 & 15 & 17 & -23 & 7 \\ 1 & -5 & 9 & -5 & -5 & 9 & -5 & 1 \\ -1 & 7 & -21 & 35 & -35 & 21 & -7 & 1 \end{bmatrix},$$

where  $\mathbf{F}_4 = \text{diag}\left(\frac{1}{2}, \frac{1}{\sqrt{20}}, \frac{1}{2}, \frac{1}{\sqrt{20}}\right)$  and  $\mathbf{F}_8 = \text{diag}\left(\frac{1}{\sqrt{2}}, \frac{1}{\sqrt{42}}, \frac{1}{\sqrt{42}}, \frac{1}{\sqrt{66}}, \frac{1}{\sqrt{142}}, \frac{1}{\sqrt{546}}, \frac{1}{\sqrt{66}}, \frac{1}{\sqrt{858}}\right)$ . We observe that  $\mathbf{T}_4$  and  $\mathbf{T}_8$  are written as a result from the product of an integer matrix and a diagonal matrix which requires float-point representation.

## 3 DTT APPROXIMATIONS AND CODING OPTIMALITY

In this section, we aim at proposing an extremely low-complexity DTT approximation. Our methodology consists of generating a class of parametric approximate matrices and then identify the optimal class member in terms of coding performance.

### 3.1 RELATED WORK

To the best of our knowledge, the only DTT approximation archived in literature was proposed in [42]. That approximation was obtained by means of a parameterization of integer functions combined with a normalization of transformation matrix columns. The derived approximation in [42] furnishes good coding capabilities, but it lacks orthogonality or near-orthogonality properties. As a consequence, the forward and inverse transformations are quite distinct and possess unbalanced computational complexities.

### 3.2 PARAMETRIC LOW-COMPLEXITY MATRICES

In [35, 36, 38, 44], DCT approximations were proposed according to following operation:

$$\text{int}(\alpha \cdot \mathbf{C}),$$

where  $\text{int}(\cdot)$  is an integer function,  $\alpha$  is a real scaling factor, and  $\mathbf{C}$  is the exact DCT matrix. Usual integer functions include the floor, ceiling, signal, and rounding functions [38]. In this work, these functions operate element-wise when applied to a matrix argument.

A similar approach is sought for the proposed DTT approximation. However, in contrast with the DCT, the rows of DTT matrix (basis vectors) have a widely varying dynamic range. Thus, the integer function may excessively penalize the rows with small dynamic range. To compensate this phenomenon, we normalize the rows of  $\mathbf{T}_4$  and  $\mathbf{T}_8$  according to left multiplications by  $\mathbf{D}_4 = \text{diag}\left(2, \frac{\sqrt{20}}{3}, 2, \frac{\sqrt{20}}{3}\right)$  and  $\mathbf{D}_8 = \text{diag}\left(\sqrt{8}, \frac{\sqrt{168}}{7}, \frac{\sqrt{168}}{7}, \frac{\sqrt{264}}{7}, \frac{\sqrt{568}}{13}, \frac{\sqrt{2184}}{23}, \frac{\sqrt{264}}{9}, \frac{\sqrt{3432}}{35}\right)$ , respectively.

The sought approximations are required to possess extremely low complexity. One way of ensuring this property is to adopt an integer function whose co-domain is a set of low-complexity integer. In the DCT literature, common sets are:  $\mathcal{P}_0 = \{\pm 1\}$  [35],  $\mathcal{P}_1 = \{0, \pm 1\}$  [36], and  $\mathcal{P}_2 = \{0, \pm 1, \pm 2\}$  [38]. Note that elements from these sets have very simple realization in hardware; implying multiplierless designs with only addition and bit-shifting operations [45].

Adopting  $\mathcal{P}_2$ , we have that a suitable integer function is given by:

$$\begin{aligned} \text{round} : [-1, 1] &\rightarrow \mathcal{P}_2 = \{0, \pm 1, \pm 2\}, \\ x &\mapsto \text{round}(\alpha \cdot x), \quad 0 < \alpha < 5/2, \end{aligned}$$

where  $\text{round}(x) = \text{sign}(x) \cdot \lfloor |x| + \frac{1}{2} \rfloor$  is the rounding function as implemented in MATLAB [46], Octave [47], and Python [48] programming languages. Following the methodology described in [38], we obtain the following parametric class of matrices:

$$\mathbf{T}_N(\alpha) = \text{round}(\alpha \cdot \mathbf{D}_N \cdot \mathbf{T}_N), \quad N \in \{4, 8\}. \quad (3)$$

### 3.3 DTT APPROXIMATION

A given low-complexity matrix  $\mathbf{T}_N(\alpha)$  can be used to approximate the DTT matrix by means of orthogonalization or quasi-orthogonalization as described in [36–38]. As a result, an approximation for  $\mathbf{T}_N$ , referred to as  $\hat{\mathbf{T}}_N(\alpha)$ , can be obtained by:

$$\hat{\mathbf{T}}_N(\alpha) = \mathbf{S}_N(\alpha) \cdot \mathbf{T}_N(\alpha), \quad (4)$$

where  $\mathbf{S}_N(\alpha) = \sqrt{\{\text{ediag}(\mathbf{T}_N(\alpha) \cdot \mathbf{T}_N(\alpha)^\top)\}^{-1}}$  is a diagonal matrix,  $\text{ediag}(\cdot)$  returns a diagonal matrix with the diagonal entries of its argument and  $\sqrt{\cdot}$  is the matrix element-wise square root operator [38]. If

$$\mathbf{T}_N(\alpha) \cdot \mathbf{T}_N(\alpha)^\top = [\text{diagonal matrix}] \quad (5)$$

holds true, then  $\hat{\mathbf{T}}_N(\alpha)$  is an orthogonal matrix [49]. Otherwise, it is possibly a near orthogonal matrix [38]. An approximation is said quasi-orthogonal when the deviation from diagonality of  $\mathbf{T}_N(\alpha) \cdot \mathbf{T}_N(\alpha)^\top$  is considered small. Let  $\mathbf{A}$  be a square real matrix. The deviation from diagonality  $\delta(\mathbf{A})$  is given by [50]:

$$\delta(\mathbf{A}) = 1 - \frac{\|\text{ediag}(\mathbf{A})\|_F}{\|\mathbf{A}\|_F},$$

where  $\|\cdot\|_F$  is the Frobenius norm for matrices [49]. In the context of image compression, a deviation from diagonality value below  $1 - \frac{2}{\sqrt{5}} \approx 0.1056$  indicates quasi-orthogonality [35, 38].

### 3.4 OPTIMIZATION PROBLEM

Now our goal is to identify in the family  $\mathbf{T}_N(\alpha)$  the matrix that furnishes the best approximation. We adopted two metrics as figures of merit to guide the optimal choice: (i) the unified coding gain  $C_g$  [51, 52] and (ii) the transform efficiency  $\eta$  [53]. These metrics are relevant, because they quantify the transform capacity of removing signal redundancy, as well as data compression and decorrelation [53].

Hence, following the methodology in [54], we propose the following multicriteria optimization problem:

$$\alpha^* = \arg \max_{0 < \alpha < 5/2} \left\{ C_g(\hat{\mathbf{T}}_N(\alpha)), \eta(\hat{\mathbf{T}}_N(\alpha)) \right\}, \quad N \in \{4, 8\},$$

where  $\alpha^*$  is the scaling parameter that results in the optimal low complexity matrix  $\mathbf{T}_N^* \triangleq \hat{\mathbf{T}}_N(\alpha^*)$  according to (3).

The above optimization problem is not analytically tractable. Thus, we resort to exhaustive numerical search to obtain  $\alpha^*$ . We consider linearly spaced values of  $\alpha$  with a step of  $10^{-3}$  in the interval  $0 < \alpha < 5/2$ . For  $N = 4$  and  $N = 8$ , we obtain that optimality is found in the intervals  $(\frac{3}{2}, \frac{5}{2})$  and  $(\frac{23}{14}, \frac{69}{34})$ , respectively. Therefore, any value of  $\alpha$  in the aforementioned intervals effects the same approximations. For operational reasons, we selected  $\alpha = 2$ . Thus, the resulting low-complexity matrices are given below:

$$\mathbf{T}_4^* = \begin{bmatrix} 1 & 1 & 1 & 1 \\ -2 & -1 & 1 & 2 \\ -1 & -1 & -1 & 1 \\ -1 & 2 & -2 & 1 \end{bmatrix} \quad \text{and} \quad \mathbf{T}_8^* = \begin{bmatrix} 1 & 1 & 1 & 1 & 1 & 1 & 1 & 1 \\ -2 & -1 & -1 & 0 & 0 & 1 & 1 & 2 \\ 2 & 0 & -1 & -1 & -1 & -1 & 0 & 2 \\ -2 & 1 & 2 & 1 & -1 & -2 & -1 & 2 \\ -1 & -2 & 0 & 1 & 1 & 0 & -2 & 1 \\ -1 & -2 & -1 & -1 & 1 & 1 & -2 & 1 \\ 0 & -1 & 2 & -1 & -1 & 2 & -1 & 0 \\ 0 & 0 & -1 & 2 & -2 & 1 & 0 & 0 \end{bmatrix}.$$

The associate optimal approximations are denoted by  $\hat{\mathbf{T}}_N^* \triangleq \hat{\mathbf{T}}_N(\alpha^*)$  and can be computed according to (4). Hence, we obtain:  $\hat{\mathbf{T}}_4^* = \text{diag}\left(\frac{1}{2}, \frac{1}{\sqrt{10}}, \frac{1}{2}, \frac{1}{\sqrt{10}}\right) \cdot \mathbf{T}_4^*$  and  $\hat{\mathbf{T}}_8^* = \text{diag}\left(\frac{1}{\sqrt{8}}, \frac{1}{\sqrt{12}}, \frac{1}{\sqrt{12}}, \frac{1}{\sqrt{20}}, \frac{1}{\sqrt{12}}, \frac{1}{\sqrt{14}}, \frac{1}{\sqrt{12}}, \frac{1}{\sqrt{10}}\right) \cdot \mathbf{T}_8^*$

## 4 EVALUATION AND COMPUTATIONAL COMPLEXITY

### 4.1 DISCUSSION

The obtained matrix  $\mathbf{T}_4^*$  satisfies (5) and therefore  $\hat{\mathbf{T}}_4^*$  is orthogonal. In fact, the proposed matrix is identical to the 4-point integer transform for H.264 encoding introduced by Malvar *et al.* [44]. Therefore, it is also an optimal approximate DTT. Because the 4-point DCT approximation matrix by Malvar *et al.* was submitted to in-depth analyses in the context of video coding [31], such results also apply to  $\mathbf{T}_4^*$ . Therefore, hereafter we focus the forthcoming discussions to the proposed 8-point approximation  $\mathbf{T}_8^*$ .

### 4.2 ORTHOGONALITY AND INVERTIBILITY

The matrix  $\mathbf{T}_8^*$  does not satisfy (5). Therefore, the associate approximation  $\hat{\mathbf{T}}_8^*$  is not orthogonal, i.e.  $(\hat{\mathbf{T}}_8^*)^{-1} \neq (\hat{\mathbf{T}}_8^*)^\top$ . As a consequence, the inverse does not inherit the low-complexity properties of  $\mathbf{T}_8^*$ . In other words, the entries of  $(\hat{\mathbf{T}}_8^*)^{-1}$  are not in  $\mathcal{P}_2$ . Hence, the proposed transform possesses asymmetrical computational costs when comparing the direct and inverse operations [55]. The inverse transformation is a much required tool,

specially for reconstruction encoded images back to the spatial domain [27, 56].

However,  $\mathbf{T}_8^* \cdot (\mathbf{T}_8^*)^\top$  has a low deviation from diagonality [38, 50]: only 0.024—roughly 4.4 times less than the deviation implied by the SDCT [35], which is taken as the standard reference. Therefore, the following approximation is valid:  $(\hat{\mathbf{T}}_8^*)^{-1} \approx (\mathbf{T}_8^*)^\top \cdot \text{diag}\left(\frac{1}{\sqrt{8}}, \frac{1}{\sqrt{12}}, \frac{1}{\sqrt{12}}, \frac{1}{\sqrt{20}}, \frac{1}{\sqrt{12}}, \frac{1}{\sqrt{14}}, \frac{1}{\sqrt{12}}, \frac{1}{\sqrt{10}}\right)$ . Moreover, since diagonal matrices can be absorbed into other computational steps [38, 40, 42],  $(\mathbf{T}_8^*)^{-1}$  can be replaced with the low-complexity matrix  $(\mathbf{T}_8^*)^\top$ . This has the advantage of using the same algorithm for both forward and inverse approximations.

#### 4.3 PERFORMANCE ASSESSMENT

The proposed approximations were compared with their corresponding exact DTT in terms of coding performance as measured according to the coding gain and the transform efficiency. For  $N = 8$ , we also include in our comparisons the DTT approximation proposed in [42]. The coding performance of the proposed approximations was evaluated according to the figures of merit  $C_g$  and  $\eta$ . Table 1 displays the results. The proposed approximations are capable of furnishing coding measures very close to the exact transformations. For comparison purposes, the exact DCT has its coding gain and transform efficiency of 8.83 dB and 93.99, respectively.

Although our goal is to derive good approximations for coding, we also analyzed the resulting approximations in terms of proximity metrics. We separated the mean square error (MSE) [57], the total energy error  $\epsilon$  [36], and the transform distortion  $d$  [58]. All these measures aim at quantifying the distance between the exact transformations and their respective approximations. Analytic expressions for the MSE and  $\epsilon$  are detailed in [54]. We also evaluated the proximity of the proposed approximations with respect to the exact DTT according to the transform distortion measure suggested in [58]. This metric was originally proposed as the DCT distortion in the context of DCT approximations and quantifies in percentage a distance between exact and approximate DCT. Adapting it for the DTT, we obtain the transform distortion as follows:

$$d(\hat{\mathbf{T}}_N^*) = \left\{ 1 - \frac{1}{N} \cdot \left\| \text{ediag} \left\{ \mathbf{T}_N \cdot (\hat{\mathbf{T}}_N^*)^\top \right\} \right\|_2^2 \right\} \times 100\%,$$

where  $\|\cdot\|_2$  is the euclidean norm for matrices [49]. Low values of distortion indicates proximity with the DTT. As a comparison for  $N = 4$ , the 4-point DCT approximation proposed in [59] has a distortion of 7.32%. Proximity results are also shown in Table 1.

#### 4.4 FAST ALGORITHM AND ARITHMETIC COMPLEXITY

Now we aim at deriving fast algorithms for the obtained DTT approximations. Being identical to the H.264 4-point DCT approximation, the derived matrix  $\mathbf{T}_4^*$  was given fast algorithms in [44]. Although  $\mathbf{T}_8^*$  is multiplication free, without a fast algorithm, its direct implementation requires 44 additions and 24 bit-shifting operations. Thus we focus our efforts on the efficient computation of  $\mathbf{T}_8^*$ . To such end, a sparse matrix factorization is sought, where the number of additions and bit-shifting operations can be significantly reduced [45, 60].

The sparse matrix factorization proposed in the manuscript was derived from scratch based on usual butterfly structures [45].

We obtained the following decomposition:

$$\mathbf{T}_8^* = \mathbf{P} \cdot \mathbf{A}_2 \cdot \mathbf{A}_1 \cdot \mathbf{B}_8,$$

where

$$\mathbf{B}_8 = \begin{bmatrix} 1 & 0 & 0 & 0 & 0 & 0 & 0 & 1 \\ 0 & 1 & 0 & 0 & 0 & 0 & 1 & 0 \\ 0 & 0 & 1 & 0 & 0 & 1 & 0 & 0 \\ 0 & 0 & 0 & 1 & 1 & 0 & 0 & 0 \\ 0 & 0 & 0 & 1 & -1 & 0 & 0 & 0 \\ 0 & 0 & 1 & 0 & 0 & -1 & 0 & 0 \\ 0 & 1 & 0 & 0 & 0 & 0 & -1 & 0 \\ 1 & 0 & 0 & 0 & 0 & 0 & 0 & -1 \end{bmatrix},$$

$$\mathbf{A}_1 = \begin{bmatrix} 0 & 0 & 1 & 0 & 0 & 0 & 0 & 0 \\ 1 & 0 & 0 & 1 & 0 & 0 & 0 & 0 \\ 0 & 1 & 0 & 0 & 0 & 0 & 0 & 0 \\ 0 & -1 & 2 & -1 & 0 & 0 & 0 & 0 \\ 2 & 0 & -1 & -1 & 0 & 0 & 0 & 0 \\ 0 & 0 & 0 & 0 & 2 & -1 & 0 & 0 \\ 0 & 0 & 0 & 0 & 1 & 1 & 0 & 0 \\ 0 & 0 & 0 & 0 & 0 & 1 & 1 & 0 \\ 0 & 0 & 0 & 0 & 0 & 0 & 2 & -1 \\ 0 & 0 & 0 & 0 & 0 & 0 & 0 & -2 \end{bmatrix},$$

$$\mathbf{A}_2 = \begin{bmatrix} 1 & 1 & 1 & 0 & 0 & 0 & 0 & 0 & 0 & 0 \\ 0 & 1 & -2 & 0 & 0 & 0 & 0 & 0 & 0 & 0 \\ 0 & 0 & 0 & 1 & 0 & 0 & 0 & 0 & 0 & 0 \\ 0 & 0 & 0 & 0 & 1 & 0 & 0 & 0 & 0 & 0 \\ 0 & 0 & 0 & 0 & 0 & 1 & 0 & 0 & 0 & 0 \\ 0 & 0 & 0 & 0 & 0 & 0 & 1 & 0 & 0 & 0 \\ 0 & 0 & 0 & 0 & 0 & 0 & 0 & 1 & 1 & 0 \\ 0 & 0 & 0 & 0 & 0 & 0 & 0 & -1 & 0 & 1 \\ 0 & 0 & 0 & 0 & 0 & 0 & 0 & -1 & 0 & 1 \end{bmatrix},$$

$$\mathbf{P} = \begin{bmatrix} 1 & 0 & 0 & 0 & 0 & 0 & 0 & 0 \\ 0 & 0 & 0 & 0 & 0 & 1 & 0 & 0 \\ 0 & 0 & 0 & 1 & 0 & 0 & 0 & 0 \\ 0 & 0 & 0 & 0 & 1 & 0 & 0 & 0 \\ 0 & 1 & 0 & 0 & 0 & 0 & 0 & 0 \\ 0 & 0 & 0 & 0 & 0 & 1 & 0 & 0 \\ 0 & 0 & 1 & 0 & 0 & 0 & 0 & 0 \\ 0 & 0 & 0 & 1 & 0 & 0 & 0 & 0 \end{bmatrix}.$$

Matrix  $\mathbf{B}_8$  represents a layer of butterfly structures,  $\mathbf{A}_1$  and  $\mathbf{A}_2$  denote additive matrices with bit-shifting operations, and  $\mathbf{P}$  represents a final permutation, which is cost-free. The resulting algorithm preserves all algebraic and coding properties of the direct computation, while requiring less arithmetic operations. Moreover, the factor of 2 of the first matrix row can be absorbed into the diagonal matrix. The obtained factorization is represented by the signal flow graph shown in Figure 1. Such algorithm reduces the arithmetic cost of the proposed approximation to only 24 additions and six bit-shifting operations.

Table 2 compares the arithmetic complexity of the discussed methods evaluated according to both their respective fast algorithms. The additive and total arithmetic complexity of the proposed approximation are 45.5% and 58.9% lower than the exact transform, respectively. Although, the computational cost of the proposed approximation is slightly higher than the *forward* DTT approximation in [42], it is important to notice that the inverse transformation in [42] is relatively more complex. Considering the combination of forward and inverse transformation, the design in [42] requires 49 additions, whereas the proposed design requires 48 additions. Bit-shifting costs are virtually null, because in a hardware implementation they represent only wiring. For comparison, the popular Loeffler DCT algorithm [61] requires 11 floating-point multiplications and 29 additions. Although the actual approximation consists of the multiplication of the low-complexity matrix and a diagonal matrix as shown in (4), the multiplications introduced by diagonal matrices represent no additional arithmetic complexity in image compression applications. This is because they can be absorbed into the image quantization step [27, 56] of JPEG-like image compression [36–41]. Furthermore, the new approximation is capable of a better coding performance and possesses one order of magnitude lower proximity measure as shown in Table 1. Therefore, both performance and arithmetic complexity measures are favorable to the proposed approximation.

## 5 IMAGE AND VIDEO COMPRESSION EXPERIMENTS

In this section, we perform two computation experiments. The first one consists of still image compression considering a JPEG

Table 1: Performance assessment

$N$	Method	$C_g$ (dB)	$\eta$	MSE	$\epsilon$	$d$	$\delta$
4	Exact DTT [26]	7.55	97.25	-	-	-	0
	Proposed	7.55	97.33	0.001	0.13	0.29%	0
8	Exact DTT [15]	8.68	92.86	-	-	-	0
	DTT Approx. [42]	6.60	83.50	0.015	3.32	12.61%	0.09
	Proposed	8.57	89.52	0.002	0.77	3.03%	0.024

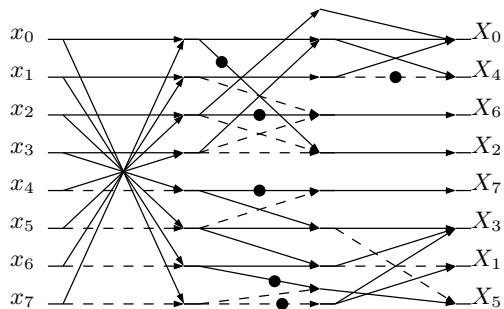


Figure 1: Signal flow graph for  $\mathbf{T}_g^*$ . Input data  $x_n$ ,  $n = 0, 1, \dots, 7$ , relates to output  $X_m$ ,  $m = 0, 1, \dots, 7$ . Dashed arrows and black nodes represent multiplications by  $-1$  and  $2$ , respectively.

Table 2: Fast algorithm arithmetic complexity comparison

Method	Mult.	Adit.	Shifts	Total
Exact DTT [15]	0	44	29	73
Forward DTT approx. [42]	0	20	0	20
Inverse DTT approx. [42]	0	29	8	37
Proposed	0	24	6	30

procedure. The second simulation assess the effectiveness of the proposed approximations under realistic video encoding conditions.

## 5.1 IMAGE COMPRESSION

We adopted the image compression method according to the JPEG standard [27, 56]. A set of 45 512×512 8-bit images were obtained from a public image bank [62] and submitted to processing. The selected images encompass a wide range of categories, including 13 textures, 12 satellite images, three human faces and several other miscellaneous scenarios. For each image, the luminance component was extracted and subdivided into 8×8 blocks,  $\mathbf{I}_{i,j}$ ,  $i, j = 1, 2, \dots, 64$ . After preprocessing, each block was submitted to the the following operation:

$$\mathbf{M}_{i,j} = \mathbf{P} \cdot \mathbf{I}_{i,j} \cdot \mathbf{P}^\top,$$

where  $\mathbf{M}_{i,j}$  is the 2-D transform-domain data and  $\mathbf{P}$  is a given 1-D transformation matrix, such as the exact or approximate DTT. Then each subblock  $\mathbf{M}_{i,j}$  was element-wise divided by a quantization matrix, yielding the quantized JPEG coefficients  $\mathbf{J}_{i,j}$ , as follows:

$$\mathbf{J}_{i,j} = \text{round}(\mathbf{M}_{i,j} \oslash \mathbf{Q}),$$

where  $\mathbf{Q} = \lfloor (S \cdot \mathbf{Q}_0 + 50)/100 \rfloor$  is the quantization matrix,  $\lfloor \cdot \rfloor$  denotes the floor function, the default quantization table is

$$\mathbf{Q}_0 = \begin{bmatrix} 16 & 11 & 10 & 16 & 24 & 40 & 51 & 61 \\ 12 & 12 & 14 & 19 & 26 & 58 & 60 & 55 \\ 14 & 13 & 16 & 24 & 40 & 57 & 69 & 56 \\ 14 & 17 & 22 & 29 & 51 & 84 & 80 & 62 \\ 18 & 22 & 37 & 56 & 68 & 109 & 103 & 77 \\ 24 & 35 & 55 & 64 & 81 & 104 & 113 & 92 \\ 49 & 64 & 78 & 87 & 103 & 121 & 120 & 101 \\ 72 & 92 & 95 & 98 & 112 & 100 & 103 & 99 \end{bmatrix},$$

$S = 5000/QF$ , if  $QF < 50$ , and  $200 - 2 \cdot QF$  otherwise, and  $QF$  is the quality factor [56]. If  $QF = 50$ , then  $\mathbf{Q} = \mathbf{Q}_0$ . Decreasing values of  $QF$  lead to higher compression ratios (with image total destruction at  $QF = 0$ ); whereas increasing values leads to lower compression ratios (with best possible quality at  $QF = 100$ ). In our experiments, we adopted  $QF$  varying from 10 to 90 in steps of 5. In the JPEG decoder, each sub-block is initially arithmetic decoded and dequantized according to:  $\hat{\mathbf{M}}_{i,j} = \mathbf{J}_{i,j} \odot \mathbf{Q}$ . Then, the sub-blocks are inverse transformed:  $\hat{\mathbf{I}}_{i,j} = \mathbf{P}^{-1} \cdot \hat{\mathbf{M}}_{i,j} \cdot \mathbf{P}^{-\top}$ .

Original and compressed images were compared for image degradation. The structural similarity index (SSIM) [63] and the spectral residual based similarity (SR-SIM) [64] were separated as image quality measures. The SSIM takes into account luminance, contrast, and the image structure to quantify the image degradation, being consistent with subjective quality measurements [65]. On its turn, the SR-SIM is based on the hypothesis that the visual saliency maps of natural images are closely related to their perceived quality. This measure could outperform several state-of-the-art figures of merit in experiments with standardized datasets [64]. We did not consider the peak signal-to-noise ratio (PSNR) as a quality measure, because it is not a suitable metric to capture the human perception of image fidelity and quality [57]. For each value of  $QF$ , we considered average measure values instead of values from particular images. This approach is less prone to variance effects and fortuitous data [36, 66]. For direct comparison, we selected the exact DTT [15], the approximation proposed in [42], and the proposed approximation. As an extra reference, we also included the results from the standard JPEG, which is based on the exact DCT. Figure 2 displays the results. For both selected measures, the proposed approximation performed very closely to the exact DTT, specially at

high compression ratios. It could outperform the DTT approximation in [42] in terms of SSIM and SR-SIM for  $QF < 80$  and  $QF < 55$ , respectively. It shows that the proposed approximation is more efficient in the scenario of high and moderate compression, which are the very common cases [67], suitable for low-power devices. The approximation in [42] could attain a better performance at low compression ratios because it satisfies the perfect reconstruction property—albeit at the expense of an inverse transformation with higher arithmetic complexity. On the other hand, the proposed approximation explores the near-orthogonality property which could excel in moderate to high compression scenarios—which are often more relevant [67].

For qualitative evaluation purposes, Figure 3 shows the compressed Lena image according to the exact DTT and the proposed approximation. We adopted the scenario of high/moderate compression with  $QF = 15$  and  $QF = 50$ , respectively. In both cases, the approximate transform was capable of producing comparable results to the exact DTT with visually similar images.

## 5.2 VIDEO COMPRESSION SIMULATION

To evaluate the proposed transform performance in video coding, we have embedded the DTT approximation in the widely used x264 software library [68] for encoding video streams into the H.264/AVC standard [31]. The default 8-point transform employed in H.264 is the following integer DCT approximation [69]:

$$\hat{\mathbf{C}} = \frac{1}{8} \cdot \begin{bmatrix} 8 & 8 & 8 & 8 & 8 & 8 & 8 & 8 \\ 12 & 10 & 6 & 3 & -3 & -6 & -10 & -12 \\ 8 & 4 & -4 & -8 & -8 & -4 & 4 & 8 \\ 10 & -3 & -12 & -6 & 6 & 12 & 3 & -10 \\ 8 & -8 & -8 & 8 & 8 & -8 & -8 & 8 \\ 6 & -12 & 3 & 10 & -10 & -3 & 12 & -6 \\ 4 & -8 & 8 & -4 & -4 & 8 & -8 & 4 \\ 3 & -6 & 10 & -12 & 12 & -10 & 6 & -3 \end{bmatrix}.$$

The fast algorithm for the above transformation requires 32 additions and 14 bit-shifting operations [69]. Therefore, the proposed 8-point transform requires 25% less additions and 57% less bit-shifting operations than the fast algorithm for  $\hat{\mathbf{C}}$ .

Eleven 300-frame common intermediate format (CIF) videos obtained from an online test video database [70] were encoded with the standard software and then with the modified software. We employed the software default settings and conducted the simulation under two scenarios: (i) target bitrate varying from 50 to 500 kbps with steps of 50 kbps and (ii) quantization parameter (QP) varying from 5 to 50 with steps of 5. Psychovisual optimization was disabled in order to obtain valid SSIM values. Besides PSNR evaluation, the discussed software library [68] offers natively SSIM measurements for video quality assessment. Average SSIM of the luma component were computed for all reconstructed frames. The results are shown in Figure 4 in terms of the absolute percentage error (APE) [38] of the SSIM with respect to the standard DCT-based transformation in the original H.264/AVC codec. This measure is given by:

$$\text{APE}(\text{SSIM}) = \left| \frac{\text{SSIM}_{\text{H.264}} - \text{SSIM}_{\mathbf{P}}}{\text{SSIM}_{\text{H.264}}} \right|,$$

where  $\text{SSIM}_{\text{H.264}}$  returns the SSIM figures as computed according to the H.264 standard and  $\text{SSIM}_{\mathbf{P}}$  represents the SSIM when the exact DTT, the approximation in [42], or the proposed approximation are considered. SSIM curves for the DCT are absent, because they were employed as performance references. The use of the proposed transform effects a minor degradation in the video quality. It also could perform better than the previous approximation in all cases.

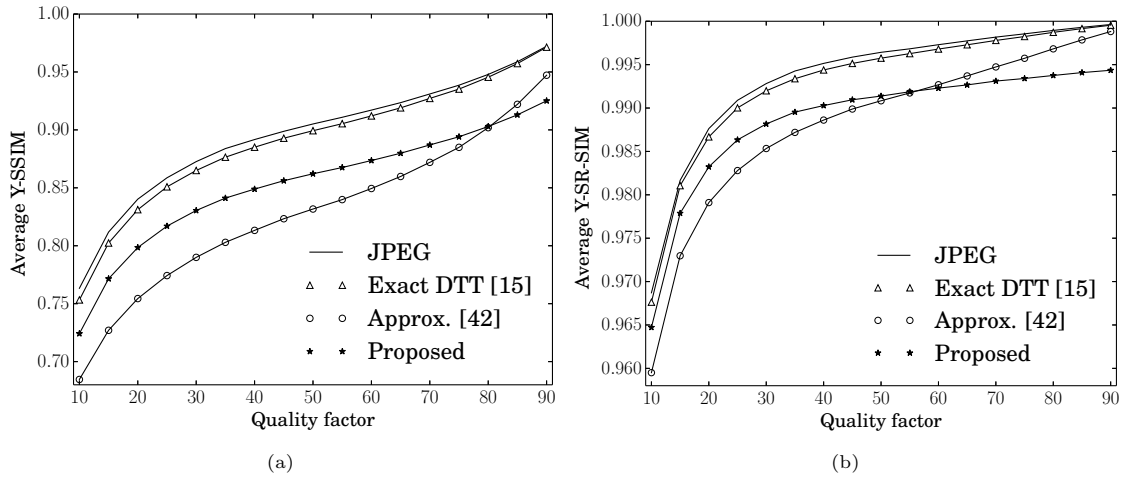


Figure 2: Average SSIM (top) and SR-SIM (bottom) measurements for image compression for the considered transforms at several values of  $QF$ .

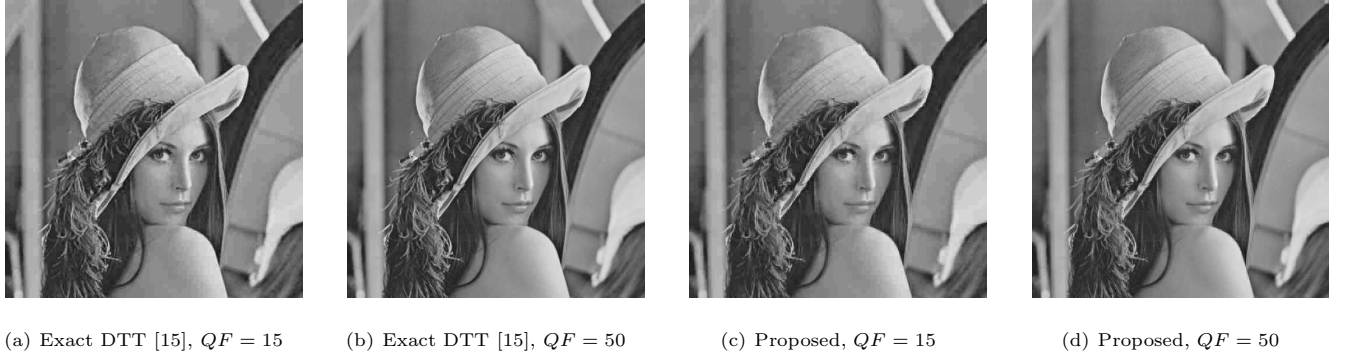


Figure 3: Compressed 'Lena' image for  $QF = 15$  and  $QF = 50$ .

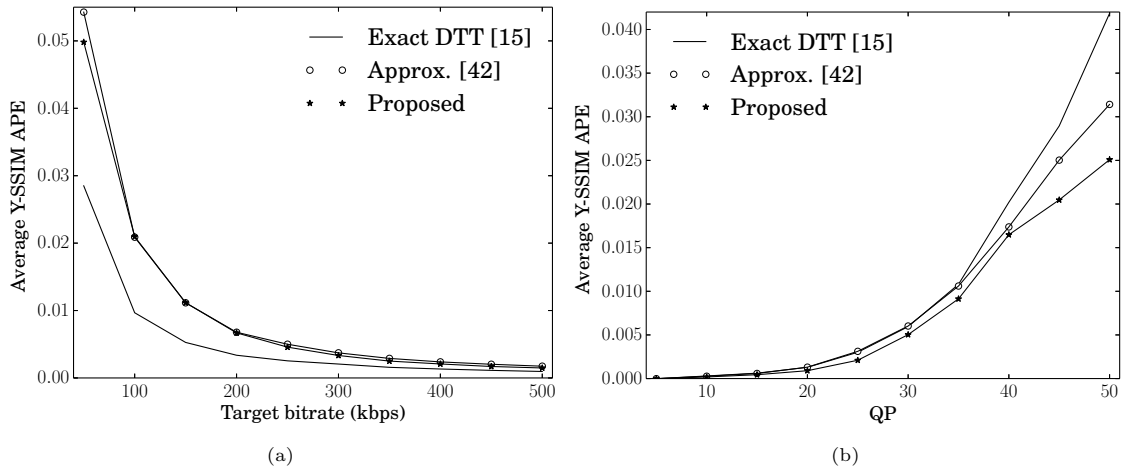


Figure 4: Video quality assessment in terms of target bitrate and QP.

Figure 5 displays the first encoded frame of two standard video sequences at low bitrate (200 kbps). The compressed frames resulting from the original and modified codecs are visually indistinguishable.

## 6 HARDWARE SECTION

To compare the hardware resource consumption of the proposed approximate DTT against the exact DTT fast algorithm proposed in [15], algorithm proposed in [42] and the Loeffler DCT [61], the 2-D version of both algorithms were initially modeled and tested in Matlab Simulink and then were physically realized on a Xilinx Virtex-6 XC6VVSX475T-1FF1759 Reconfigurable Open Architecture Computing Hardware-2 (ROACH2) board [71]. The ROACH2 board consists of a Xilinx Virtex 6 FPGA, 16 complex analog-to-digital converters (ADC), multi-gigabit transceivers and a 72-bit DDR3 RAM.

The 1-D versions were initially modeled and the 2-D versions were generated using two 1-D designs along with a transpose buffer. Designs were verified using more than 10000 test vectors with complete agreement with theoretical values. Results are shown in Table 3. Metrics, including configurable logic blocks (CLB) and flip-flop (FF) count, critical path delay ( $T_{cpd}$ , in ns), and maximum operating frequency ( $F_{max}$ , in MHz) are provided. The percentage reduction in the number of CLBs and FFs were 43.2% and 25.0%, respectively, compared with the exact DTT fast algorithm proposed in [15]. It is important to emphasize that the approximation in [42] is asymmetric; the forward and inverse transform possess different structures, being the inverse operation more complex (cf. Table 2). For comparisons, we adopt the average measurement between forward and inverse realizations. The proposed approximation could provide higher maximum operating frequency with improvements of 85.9%, 43.5%, and 9.7% when compared to the Loeffler DCT [61], the exact DTT [15], and the design in [42], respectively.

The ASIC realization was done by porting the hardware description language code to 0.18 um CMOS technology and was subjected to synthesis and place-and-route according to the Cadence Encounter Digital Implementation (EDI) for AMS libraries. Libraries for the best case scenario were employed in getting the place-and-route results with gate voltage of 1.8 V. The adopted figures of merit for the ASIC synthesis were: area ( $A$ ) in  $\text{mm}^2$ , area-time complexity ( $AT$ ) in  $\text{mm}^2 \cdot \text{ns}$ , area-time-squared complexity ( $AT^2$ ) in  $\text{mm}^2 \cdot \text{ns}^2$ , dynamic ( $D_p$ ) power consumption in  $\text{mW}/\text{MHz}$ , critical path delay ( $T_{cpd}$ ) in ns, and maximum operating frequency ( $F_{max}$ ) in MHz. Results are displayed in Table 4. The figures of merit  $AT$  and  $AT^2$  had percentage reductions of 57.7% and 57.4% when compared with the exact DTT. Thus, the proposed design could attain reductions of 17.3%, 20.6%, and 82.1% for area,  $AT^2$ ,  $T_{cpd}$ , and dynamic power consumption, respectively, when compared to [42].

## 7 DISCUSSION AND CONCLUSION

In this work, a low-complexity near-orthogonal 8-point DTT approximation suitable for image and video coding was proposed. A fast algorithm for proposed DTT approximation which requires only 24 additions and six bit-shifting operations was also introduced. This fast algorithm can be used for both forward and near inverse transformations. The additive arithmetic cost of the proposed approximation is 45.5% and 2.05% lower when compared with the exact DTT fast algorithm and the

DTT approximation in [42], respectively. Moreover, the proposed transform exhibited similar coding performance with the exact DTT and outperformed previous approximations [42] according to computational experiments with popular visual image compression standards. In terms of video coding, the results from the proposed tool were virtually indistinguishable from the ones furnished by the approximation in [42]. Thus, the new tool outperforms the competing methods both in computational cost and coding performance. The proposed method was embedded into the JPEG standard and the standard software library for H.264/AVC video coding. Obtained results showed negligible degradation when compared to the standard DCT-based compression methods in both cases. The 2-D versions were realized in FPGA using ROACH2 hardware platform and ASIC place and route was realized using Cadence encounter with AMS standard cells and the results show a 43.1% reduction in the number of CLB for the FPGA realization and a 57.7% reduction in area-time figure for the ASIC place and route realization when compared with the exact DTT. The proposed design could excel in providing high operation frequency and very low power consumption. Therefore, the proposed approximation offers low computational complexity while maintaining good coding performance. Systems that operate under low processing constraints and require video streaming can benefit of the proposed low-complexity codecs and low-power hardware. In particular, applications in the following contexts meet such requirements that need low-complexity [72]: environmental monitoring, habitat monitoring, surveillance, structural monitoring, equipment diagnostics, disaster management, and emergency response [73].

## ACKNOWLEDGMENT

Arjuna Madanayake thanks the Xilinx University Program (XUP) for the Xilinx Virtex-6 Sx475 FPGA device installed in on the ROACH2 board.

## REFERENCES

- [1] A. F. Nikiforov, S. K. Suslov, and V. B. Uvarov, *Classical Orthogonal Polynomials of a Discrete Variable*, ser. Springer Series in Computational Physics. Springer Berlin Heidelberg, 1991.
- [2] P. D. Draznev and E. B. Saff, "Constrained energy problems with applications to orthogonal polynomials of a discrete variable," *Journal d'Analyse Mathématique*, vol. 72, pp. 223–259, 1997. [Online]. Available: <http://dx.doi.org/10.1007/BF02843160>
- [3] M. Cãmara, J. Fábrega, M. A. Fiol, and E. Garriga, "Some families of orthogonal polynomials of a discrete variable and their applications to graphs and codes," *The Electronic Journal of Combinatorics*, vol. 16, pp. 1–30, 2009.
- [4] H. Zhu, M. Liu, H. Shu, H. Zhang, and L. Luo, "General form for obtaining discrete orthogonal moments," *IET Image Processing*, vol. 4, pp. 335–352, Oct 2010.
- [5] A. Goshtasby, "Template matching in rotated images," *IEEE Transactions on Pattern Analysis and Machine Intelligence*, vol. 7, no. 3, pp. 338–344, May 1985.
- [6] M. I. Heywood and P. D. Noakes, "Fractional central moment method for movement-invariant object classification," *IEE Proceedings—Vision, Image and Signal Processing*, vol. 142, no. 4, pp. 213–219, Aug 1995.
- [7] V. Markandey and R. I. P. de Figueiredo, "Robot sensing techniques based on high-dimensional moment invariants and tensors," *IEEE Transactions on Robotics and Automation*, vol. 8, no. 2, pp. 186–195, Apr 1992.
- [8] R. Mukundan, S. H. Ong, and R. A. Lee, "Image analysis by Tchebichef moments," *IEEE Transactions on Image Processing*, vol. 10, pp. 1357–1364, 2001.
- [9] L. Leida, Z. Hancheng, Y. Gaobo, and Q. Jiansheng, "Referenceless measure of blocking artifacts by Tchebichef kernel analysis," *IEEE Signal Processing Letters*, vol. 21, no. 1, pp. 122–125, Jan 2014.



Figure 5: First frame of the compressed ‘Foreman’ sequence, with a target bitrate of 200 kbps.

Table 3: Hardware resource consumption using Xilinx Virtex-6 XC6VVSX475T 1FF1759 device

Method	CLB	FF	$T_{cpd}$ (ns)	$F_{max}$ (MHz)
Exact DTT [15]	2941	7271	7.688	130.07
Approximation in [42]	1515	6058	5.596	178.69
Inverse Approximation in [42]	1713	4834	6.184	161.71
Loeffler DCT [61]	3250	4413	9.956	100.44
Proposed DTT	1671	5455	5.356	186.70

Table 4: Hardware resource consumption for CMOS 0.18 um ASIC place and route

FRS Method	Area (mm <sup>2</sup> )	$AT$	$AT^2$	$T_{cpd}$ (ns)	$F_{max}$ (MHz)	$D_p$ (mW/MHz)
Exact DTT [15]	0.872	3.84	16.92	4.405	227.01	0.182
Approximation in [42]	0.237	1.34	7.52	5.635	177.46	0.171
Inverse Approximation in [42]	0.323	1.79	9.89	5.536	180.64	0.724
Loeffler DCT [61]	0.684	4.20	25.85	6.148	162.65	1.961
Proposed	0.366	1.62	7.20	4.434	225.53	0.080

- [10] J.-L. Rose, C. Revol-Muller, D. Charpigny, and C. Odet, "Shape prior criterion based on Tchebichef moments in variational region growing," in *2009 16th IEEE International Conference on Image Processing (ICIP)*, Nov 2009, pp. 1081–1084.
- [11] H. Zhang, X. Dai, P. Sun, H. Zhu, and H. Shu, "Symmetric image recognition by Tchebichef moment invariants," in *2010 17th IEEE International Conference on Image Processing (ICIP)*, Sept 2010, pp. 2273–2276.
- [12] Q. Li, H. Zhu, and Q. Liu, "Image recognition by combined affine and blur Tchebichef moment invariants," in *2011 4th International Congress on Image and Signal Processing (CISP)*, vol. 3, Oct 2011, pp. 1517–1521.
- [13] H. Huang, G. Coatrieux, H. Shu, L. Luo, and C. Roux, "Blind integrity verification of medical images," *IEEE Transactions on Information Technology in Biomedicine*, vol. 16, no. 6, pp. 1122–1126, Nov 2012.
- [14] S. Ishwar, P. K. Meher, and M. N. S. Swamy, "Discrete Tchebichef transform—a fast  $4 \times 4$  algorithm and its application in image/video compression," in *2008 IEEE International Symposium on Circuits and Systems (ISCAS)*, 2008, pp. 260–263.
- [15] S. Prattipati, S. Ishwar, P. K. Meher, and M. N. S. Swamy, "A fast  $8 \times 8$  integer Tchebichef transform and comparison with integer cosine transform for image compression," in *2013 IEEE 56th International Midwest Symposium on Circuits and Systems (MWSCAS)*, 2013, pp. 1294–1297.
- [16] N. A. Abu, S. L. Wong, N. Herman, and R. Mukundan, "An efficient compact Tchebichef moment for image compression," in *2010 10th International Conference on Information Sciences Signal Processing and their Applications (ISSPA)*, May 2010, pp. 448–451.
- [17] Q. Li and H. Zhu, "Block-based compressed sensing of image using directional Tchebichef transforms," in *2012 IEEE International Conference on Systems, Man, and Cybernetics (SMC)*, Oct 2012, pp. 2207–2212.
- [18] R. K. Senapati, U. C. Pati, and K. K. Mahapatra, "Reduced memory, low complexity embedded image compression algorithm using hierarchical listless discrete Tchebichef transform," *IET Image Processing*, vol. 8, no. 4, pp. 213–238, Apr 2014.
- [19] N. Ahmed, T. Natarajan, and K. R. Rao, "Discrete cosine transform," *IEEE Transactions on Computers*, vol. C-23, no. 1, pp. 90–93, Jan. 1974.
- [20] F. Ernanwan, N. A. Abu, and N. Suryana, "TMT quantization table generation based on psychovisual threshold for image compression," in *2013 International Conference of Information and Communication Technology (ICoICT)*, Mar 2013, pp. 202–207.
- [21] R. K. Senapati, U. C. Pati, and K. K. Mahapatra, "A low complexity embedded image coding algorithm using hierarchical listless DTT," in *2011 8th International Conference on Information, Communications and Signal Processing (ICICSP)*, Dec 2011, pp. 1–5.
- [22] F. Ernanwan, E. Noersasongko, and N. A. Abu, "An efficient  $2 \times 2$  Tchebichef moments for mobile image compression," in *2011 International Symposium on Intelligent Signal Processing and Communications Systems (ISPACS)*, Dec 2011, pp. 1–5.
- [23] L. W. Chew, L.-M. Ang, and K. P. Seng, "Survey of image compression algorithms in wireless sensor networks," in *2008 International Symposium on Information Technology (ITSim)*, vol. 4, Aug 2008, pp. 1–9.
- [24] M. Guo, M. H. Ammar, and E. W. Zegura, "V3: a vehicle-to-vehicle live video streaming architecture," in *2005 3rd IEEE International Conference on Pervasive Computing and Communication (PerCom)*, Mar 2005, pp. 171–180.
- [25] D. H. Friedman, "Streaming implementation of video algorithms on a low-power parallel architecture," in *2013 IEEE Global Conference on Signal and Information Processing (GlobalSIP)*, Dec 2013, pp. 650–653.
- [26] K. Nakagaki and R. Mukundan, "A fast  $4 \times 4$  forward discrete Tchebichef transform algorithm," *IEEE Signal Processing Letters*, vol. 14, pp. 684–687, 2007.
- [27] G. K. Wallace, "The JPEG still picture compression standard," *IEEE Transactions on Consumer Electronics*, vol. 38, no. 1, pp. xviii–xxxiv, Feb 1992.
- [28] International Organisation for Standardisation, "Generic coding of moving pictures and associated audio information part 2: Video, ISO/IEC JTC1/SC29/WG11 coding of moving pictures and audio," 1994.
- [29] International Telecommunication Union, "ITU-T recommendation H.261 version 1: Video codec for audiovisual services at  $p \times 64$  kbits," Technical Report, ITU-T, 1990.
- [30] —, "ITU-T recommendation H.263 version 1: Video coding for low bit rate communication," Technical Report, ITU-T, 1995.
- [31] I. Richardson, *The H.264 Advanced Video Compression Standard*, 2nd ed. John Wiley and Sons, 2010.
- [32] G. J. Sullivan, J. Ohm, W.-J. Han, and T. Wiegand, "Overview of the high efficiency video coding (HEVC) standard," *IEEE Transactions on Circuits and Systems for Video Technology*, vol. 22, pp. 1649–1668, 2012.
- [33] F. Bossen, B. Bross, K. Suhring, and D. Flynn, "HEVC complexity and implementation analysis," *IEEE Transactions on Circuits and Systems for Video Technology*, vol. 22, no. 12, pp. 1685–1696, Dec 2012.
- [34] Google Inc., "VP9," The WebM Project, <http://www.webmproject.org/vp9/>, 2015.
- [35] T. I. Haweel, "A new square wave transform based on the DCT," *Signal Processing*, vol. 81, pp. 2309–2319, 2001. [Online]. Available: <http://www.sciencedirect.com/science/article/pii/S0165168401001062>
- [36] R. J. Cintra and F. M. Bayer, "A DCT approximation for image compression," *IEEE Signal Processing Letters*, vol. 18, no. 10, pp. 579–582, Oct 2011.
- [37] F. M. Bayer and R. J. Cintra, "DCT-like transform for image compression requires 14 additions only," *Electronics Letters*, vol. 48, no. 15, pp. 919–921, July 2012.
- [38] R. J. Cintra, F. M. Bayer, and C. J. Tablada, "Low-complexity 8-point DCT approximations based on integer functions," *Signal Processing*, vol. 99, pp. 201–214, 2014. [Online]. Available: <http://www.sciencedirect.com/science/article/pii/S0165168413005161>
- [39] S. Bouguezel, M. O. Ahmad, and M. N. S. Swamy, "Low-complexity  $8 \times 8$  transform for image compression," *Electronics Letters*, vol. 44, no. 21, pp. 1249–1250, Oct 2008.
- [40] —, "A low-complexity parametric transform for image compression," in *2011 IEEE International Symposium on Circuits and Systems (ISCAS)*, May 2011, pp. 2145–2148.
- [41] —, "Binary discrete cosine and hartley transforms," *IEEE Transactions on Circuits and Systems I: Regular Papers*, vol. 60, no. 4, pp. 989–1002, Apr 2013.
- [42] P. A. M. Oliveira, R. J. Cintra, F. M. Bayer, S. Kulasekera, and A. Madanayake, "A discrete Tchebichef transform approximation for image and video coding," *IEEE Signal Processing Letters*, vol. 22, no. 8, pp. 1137–1141, Aug 2015.
- [43] H. Bateman and A. Erdélyi, *Higher transcendental functions*. McGraw-Hill, 1953, vol. 2. [Online]. Available: <http://books.google.com.br/books?id=pJQAAAAMAAJ>
- [44] H. S. Malvar, A. Hallapuro, M. Karczewicz, and L. Kerofsky, "Low-complexity transform and quantization in H.264/AVC," *IEEE Transactions on Circuits and Systems for Video Technology*, vol. 13, no. 7, pp. 598–603, Jul 2003.
- [45] R. Blahut, *Fast Algorithms for Signal Processing*. Cambridge University Press, 2010.
- [46] MATLAB, "version 8.1 (R2013a) documentation," Natick, MA, 2013.
- [47] J. W. Eaton, D. Bateman, S. Hauberg, and R. Wehbring, *GNU Octave version 3.8.0 Documentation*, 3rd ed. Free Software Foundation, Inc., Feb 2011.
- [48] Python, "version 2.7.6 documentation," Delaware, US, 2015.
- [49] G. A. F. Seber, *A Matrix Handbook for Statisticians*, ser. Wiley Series in Probability and Mathematical Statistics. Hoboken, NJ: John Wiley and Sons, Inc., 2008.
- [50] B. N. Flury and W. Gautschi, "An algorithm for simultaneous orthogonal transformation of several positive definite symmetric matrices to nearly diagonal form," *SIAM Journal on Scientific and Statistical Computing*, vol. 7, no. 1, pp. 169–184, Jan. 1986. [Online]. Available: <http://dx.doi.org/10.1137/0907013>
- [51] V. K. Goyal, "Theoretical foundations of transform coding," *IEEE Signal Processing Magazine*, vol. 18, no. 5, pp. 9–21, Sept 2001.
- [52] J. Katto and Y. Yasuda, "Performance evaluation of sub-band coding and optimization of its filter coefficients," *Journal of Visual Communication and Image Representation*, vol. 2, pp. 303–313, 1991. [Online]. Available: <http://www.sciencedirect.com/science/article/pii/1047320391900114>
- [53] V. Britanak, P. C. Yip, and K. R. Rao, *Discrete Cosine and Sine Transforms*. Academic Press, 2007. [Online]. Available: <http://books.google.com.br/books?id=iRlQHCK-rkC>
- [54] C. J. Tablada, F. M. Bayer, and R. J. Cintra, "A class of DCT approximations based on the Feig–Winograd algorithm," *Signal Processing*, vol. 113, pp. 38–51, 2015.

- [55] R. J. Cintra, H. M. Oliveira, and C. O. Cintra, "The rounded Hartley transform," in *Proceedings of the IEEE International Telecommunications Symposium-ITS'2002*, Sept 2002, pp. 1357–1364.
- [56] W. B. Pennebaker and J. L. Mitchell, *JPEG: Still Image Data Compression Standard*, ser. Chapman & Hall digital multimedia standards series. Springer, 1993.
- [57] Z. Wang and A. C. Bovik, "Mean squared error: Love it or leave it? a new look at signal fidelity measures," *IEEE Signal Processing Magazine*, vol. 26, no. 1, pp. 98–117, Jan 2009.
- [58] C.-K. Fong and W.-K. Cham, "LLM integer cosine transform and its fast algorithm," *IEEE Transactions on Circuits and Systems for Video Technology*, vol. 22, no. 6, pp. 844–854, Jun 2012.
- [59] F. M. Bayer, R. J. Cintra, A. Madanayake, and U. S. Potluri, "Multiplierless approximate 4-point DCT VLSI architectures for transform block coding," *Electronics Letters*, vol. 49, no. 24, pp. 1532–1534, Nov 2013.
- [60] A. V. Oppenheim and R. W. Schaffer, *Discrete-time signal processing*, 3rd ed., ser. Prentice-Hall signal processing series. Prentice Hall, 2010.
- [61] C. Loeffler, A. Ligtenberg, and G. S. Moschytz, "A practical fast 1-D DCT algorithms with 11 multiplications," in *IEEE International Conference on Acoustics, Speech, and Signal Processing*, vol. 2, May 1989, pp. 988–991.
- [62] University of Southern California, Signal and Image Processing Institute, "The USC-SIPI image database," <http://sipi.usc.edu/database/>, 2015.
- [63] Z. Wang, A. C. Bovik, H. R. Sheikh, and E. P. Simoncelli, "Image quality assessment: from error visibility to structural similarity," *IEEE Transactions on Image Processing*, vol. 13, no. 4, pp. 600–612, Apr 2004.
- [64] L. Zhang and H. Li, "SR-SIM: A fast and high performance IQA index based on spectral residual," in *2012 19th IEEE International Conference on Image Processing (ICIP)*, Sep 2012, pp. 1473–1476.
- [65] Z. Wang and A. C. Bovik, "Reduced- and no-reference image quality assessment," *IEEE Signal Processing Magazine*, vol. 28, no. 6, pp. 29–40, Nov 2011.
- [66] S. M. Kay, *Fundamentals of Statistical Signal Processing, Volume I: Estimation Theory*, ser. Prentice Hall Signal Processing Series. Upper Saddle River, NJ: Prentice-Hall, 1993, vol. 1.
- [67] R. Pandit, N. Khosla, G. Singh, , and H. Sharma, "Image compression and quality factor in case of JPEG image format," *International Journal of Advanced Research in Computer and Communication Engineering*, vol. 2, pp. 2578–2581, Jul 2013.
- [68] x264 team, "x264," <http://www.videolan.org/developers/x264.html>, 2015.
- [69] S. Gordon, D. Marpe, and T. Wiegand, "Simplified use of 8x8 transform—updated proposal and results," Joint Video Team (JVT) of ISO/IEC MPEG and ITU-T VCEG, doc. JVT-K028, Munich, Germany, Mar 2004.
- [70] "Xiph.org Video Test Media," <https://media.xiph.org/video/derf/>, 2015.
- [71] (2015) ROACH2. <https://casper.berkeley.edu>.
- [72] I. F. Akyildiz, T. Melodia, and K. R. Chowdhury, "A survey on wireless multimedia sensor networks," *Computer Networks*, vol. 51, pp. 921–960, 2007.
- [73] N. Kimura and S. Latifi, "A survey on data compression in wireless sensor networks," in *2005 International Conference on Information Technology: Coding and Computing (ITCC)*, vol. 2, Apr 2005, pp. 8–13.